Torque Vectoring in Electric Vehicles with In-wheel Motors

TORQUE VECTORING IN ELECTRIC VEHICLES WITH IN-WHEEL MOTORS

Henrique de Carvalho Pinheiro[0000-0001-8116-336X], Alessandro Messana[0000-0002-2350-6149], Lorenzo Sisca[0000-0002-3021-7863], Alessandro Ferraris[0000-0003-0712-3399], Andrea Giancarlo Airale[0000-0002-6857-1008], Massimiliana Carello[0000-0003-2322-0340]

Politecnico di Torino, Corso Duca degli Abruzzi 24, Torino, Italy
massimiliana.carello@polito.it

Abstract: The scope of this article is to assess the performance of a torque vectoring control strategy applied to an Innovative Hybrid Electric Vehicle with In-Wheel Electric Motors. The vehicle used in the analysis is the XAM, a two-passenger lab prototype, with a modified powertrain to simulate three drivetrain configurations: AWD, FWD and RWD. The vehicle dynamics simulation is done with Adams Car and a co-simulation in MATLAB carries out the PI controller and torque allocation functions. In this virtual environment, several standard maneuvers (such as step steering, ramp steering and double lane changes) were performed in order to tune the control gains and verify the enhancement of the dynamic response of the vehicle. The system shall be considered successful if, when compared to the baseline model (without torque vectoring control), it increases vehicle responsiveness, reinforce stability and creates a more intuitive steering, without jeopardizing other performance indicators.

Keywords: Vehicle Dynamics, Control Strategy, Multi-Body Simulation, Hybrid Electric Vehicles.

1 Objectives

Nowadays, thanks to actual electrification trends in the automotive world, several powertrain architecture and control strategies are under evaluation. The compactness of electric motors allows car makers to innovate the vehicle packaging and drivetrain architectures [1–3]. On the other side the limited amount of energy on batteries and their shape has a great impact on the design of chassis as well as on their controls and on their performance [4, 5]. The use of individual motors for each wheel allows the implementation of an effective torque vectoring control to tune the vehicle's handling in steady state and transient. If made with in-wheel motors, the packaging it is improved also because of less space required by the powertrain [6]. Information from different sensors on the car such as the accelerometer for longitudinal and lateral acceleration, gyroscope for yaw rate, Throttle Position Sensor (TPS), steering wheel angle sensor and wheel speed sensor go to an electronic control unit (Processor). The torque vectoring algorithm estimates the necessary vehicle states (such as vehicle side-slip angle β) and calculates how much torque to apply to the left and right wheels. This information is fed to the inverters, which drive the electric motors.
The subject vehicle of the article is the XAM [7], the prototype built by the research team. The general characteristics of the vehicle are summarized in Table 1.

The main objectives of direct yaw moment controls are to increase vehicle stability at critical conditions, enhance vehicle response, linearize vehicle lateral acceleration response and minimize vehicle behavior variation with longitudinal acceleration [6] [1]. Potential targets for a torque vectoring controller are to increase the maximum lateral acceleration, to

increase the linear region, and to increase steering responsiveness by decreasing the understeer gradient.

Table 1. XAM basic data

Parameter	Value
Vehicle mass (m)	450 kg
Vehicle yaw moment of inertia (I_{zz})	1560 kg.m^2
Distance front-axle to CG (a)	0.85 m
Distance CG to rear-axle (b)	1.05 m
Front and rear track width (t_f and t_r)	1.185 m
Front cornering stiffness ($C_{\alpha f}$)	41.3 kN/rad
Rear cornering stiffness ($C_{\alpha r}$)	35.4 kN/rad
Tire size	235/60R16

These controllers function in basically three tasks: the reference yaw rate generation, the control algorithm (PI controller) and the control allocation (to assign the individual torque to each of the wheels). The control scheme is shown in Figure 1.

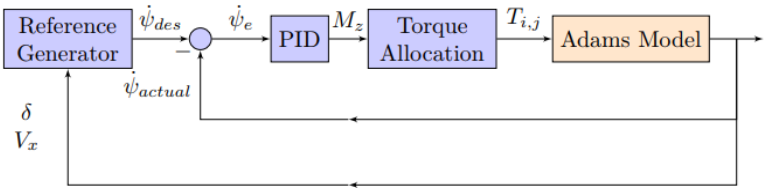

Fig. 1. Control and simulation basic scheme

2 Modelling

2.1 Multibody Model – Adams Car

As a standard *Adams Car* full vehicle assembly, the vehicle consists of, basically, 8 subsystems: tires (front/rear) and brake; suspensions (front/rear) and steering; chassis and powertrain.

The tire is modeled using the Pacejka 2002 model inside *Adams Car*. The suspension subsystems were made based on the existing *Adams Car* templates that were then modified for the proper hardpoints, springs, and dampers and to account for the IWMs inertia. With the IWMs, the motor torque is applied in the hub, which rotates around the upright and together with the wheel. In this way, the hub is connected via a revolute joint with the upright and a fix joint with the wheel. A Control System called "Torque Control" was created inside the powertrain subsystem. In it, were defined the different transducer signals for the controller

to work (such as longitudinal speed, yaw rate, steering wheel angle) and also some auxiliary signals (such as longitudinal slip ratio) that help the development of the controller. The communication interval between the *Simulink* solver and the *Adams Car* was set to 0.01. Also regarding the powertrain subsystem, for the *Adams Car* driving machine to work properly, the torque-speed map of the motor must be given to the solver in the motor parameters so the calculation for the throttle input in the simulations can be done.

2.2 Reference Generator

To generate the reference yaw rate for the controller, the most used expression is the one for steady state cornering derived from the 2-wheeled planar 'bicycle model' as seen in Equation 1:

$$\dot{\psi}_{des} = \frac{V_x}{(a+b)+K_u.V_x{}^2} \,.\, \delta \qquad (1)$$

The expression depends on the value of K_u, that can be written as in Equation 2.

$$K_u = \frac{m}{l} \,.\left(\frac{b}{C_{\alpha f}} - \frac{a}{C_{\alpha r}}\right) \qquad (2)$$

Changing K_u, the car's response is changed: increasing it induces understeer and decreasing it induces oversteer [8]. However, due to limitations of tire friction potential, the desired yaw rate described in Equation 1 is not always reachable. The vehicle cannot obtain the desired yaw rate where the tire friction is not able to provide the necessary forces. The lateral motion, lateral acceleration, must be bounded by the tire-road coefficient μ [3]. This can be expressed with:

$$a_y = V \,.\, \dot{\psi} + a_x \,.\, tan\delta + \frac{V \,.\, \dot{\beta}}{\sqrt{1+tan\,\beta^2}} \leq \mu \,.\, g \qquad (3)$$

2.3 Control Law - PI Controller

The controller consists in the calculation of the error signal, the PI controller and the calculation for the required yaw moment. The goal of the controller is to correctly track the yaw reference and minimize the error. In this part, the control law is implemented with the appropriate controller gains (K_p and K_i) to correctly track the yaw reference (generated previously) and minimize the error. The error signal can be defined as Equation 4.

$$\dot{\psi}_{error} = \dot{\psi}_{ref} - \dot{\psi}_{actual} \qquad (4)$$

$$M_z = K_p \,.\, \dot{\psi}_{error} + K_i \int \dot{\psi}_{error}\, dt \qquad (5)$$

The gains of the PI controller are virtually tuned using step steer, ramp steer and a double lane change maneuver at four different velocities (30, 60, 90 and 120 km/h). Therefore, the controller gains were tuned for each speed set point and a look-up table was built for an interpolating function between the speed set points.

2.4 Powertrain Model, Torque Allocation and Constrains

To adequately choose the in-wheel motor, requirements were made considering the purpose of the studied vehicle (small city car): Maximum speed of 120km/h in level road; continuous speed of 30km/h at 30% inclination; and transient acceleration of 2m/s 2 at 15% inclination. The chosen motor was the *Emrax* 208 Low Voltage air-cooled. It is an axial flux permanent magnet synchronous motor. Data for this motor is readily available from the manufacturer.
The motor is modeled in the *Simulink* model with a look-up table for the torque curve. Permanent magnet synchronous motors internal dynamics are much faster than the vehicle dynamics [10]. As in [11], they will be neglected with the assumption that a successful torque controller for the motors is implemented.
Torque will be divided equally between left and right, in this way all tires participate equally in the generation of the corrective yaw moment and vehicle speed will not be influenced. θ_f and θ_r indicate how much of the yaw torque is applied by the front wheels and how much by the rear wheels. In this study $\theta_f = \theta_r = 50\%$ were used, which means the torque is equally split between the front and rear.
Besides the controller design, it is also necessary to take into account the limitations and saturations of the real application. Three considerations must be made when calculating the final torque applied by the motors at the wheels: the driver's throttle demand must be satisfied, the motor torque T_{motor} should not be higher than the motor limit T_{max} for the given wheel speed rotation ω and the applied torque at the wheel should not be higher than the maximum torque the tire can handle and should not induce tire spin. The torque demand from the driver T_d is calculated with the motors look-up table as if there wasn't any torque vectoring controller. To these values, the required ΔT_{motor} from the controller are added. Finally, the values are then compared with the maximum available motor torque (throttle = 100%) at that wheel speed ω to account for the motor saturation.
After that, it is necessary to include the tire saturation to prevent wheel slip. A higher torque than the maximum tire capability should not be applied. Normal forces on each tire were calculated and the maximum longitudinal force was determined using the tire-road longitudinal friction coefficient μ_x and an effective tire rolling radius r. To find the normal forces on each tire, calculations were done based on lateral and longitudinal load transfer assuming a steady state condition and the validity of the superposition principle [9]. Aerodynamic load transfer will be neglected as aerodynamic effects are negligible for this vehicle ($C_l \sim 0$).

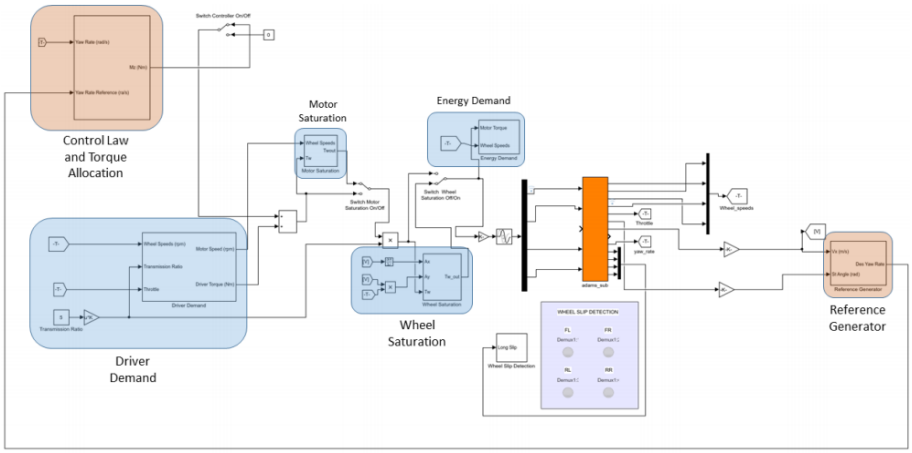

Fig. 2. Control and simulation full scheme

3 Simulation Results

Different virtual simulations were performed to tune and analyze the performance of the controller. Step steer simulations address the behavior in transients. Ramp steer and constant radius cornering simulations were done with a slow steer input to assess the controller action in a quasi-steady state condition. Double lane change and other simulations evaluate the behavior in more specific maneuvers. First, the controller performance with the AWD vehicle has been analyzed. Then, comparisons have been made with the FWD and RWD configurations. The performance of the controller has been evaluated in its capability to reach the reference value, the overshoot and settling time of the response and the instability generated by the additional yaw moment, increasing the side slip angle β. PID gains were manually tuned, the Ku reference value was chosen small, to give additional responsiveness to the vehicle. In the plots, the blue dashed curves refer to the baseline vehicle (without the torque vectoring controller) and the red solid curves refer to the controlled vehicle (with the torque vectoring).

For the step steer maneuver the simulation was done in four different speeds (30, 60, 90 and 120 km/h) with Steer angles inputs (50, 17, 9 and 6 deg) to evaluate the performance in several speed points at a low lateral acceleration condition (around 0.45 g in the baseline vehicle). The controller focus is increase responsiveness.

At 120km/h, the controller intervention is the clearest. An increase in the steady-state yaw rate, faster settling time and lower overshoot make the controlled vehicle very responsive. There is a higher curvature gain (lower radius of curvature) and lateral acceleration gain, due to the reduction of the understeer behavior of the vehicle.

It does achieve the steady-state value of the reference at 0.7s with a slight overshoot of 2%. A positive M_z is required to increase vehicle yaw rate and response. The controller, however, increases the longitudinal slip angle (Figure 4), which could cause instability if it is over a safe value, due to tire saturation.

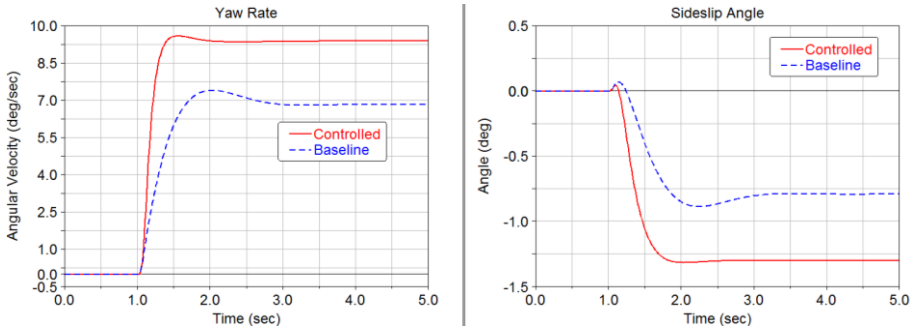

Fig. 3. Yaw rate and Sideslip Angle in 120km/h step steering

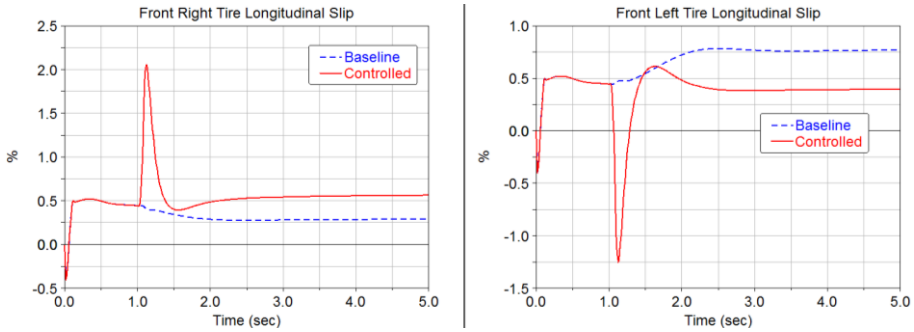

Fig. 4. Front axle Longitudinal Slip in 120 km/h step steering

A new simulation with a steering wheel angle input of δ = 15deg at V = 90km/h (resulting in a lateral acceleration of ay = 0.9g on the controlled vehicle) was done to assess the influence of a higher lateral acceleration in the controller performance.

The focus in this condition is to give stability to the vehicle and avoid rolling over.It is clear the higher difficulty to the controller to keep the vehicle stable at the higher lateral acceleration loads.

The tires of the controlled vehicle are now operating at the limits of lateral slip adhesion. For this steering input, the baseline vehicle does not reach a lateral acceleration higher than 0.7g and thus does not reach this condition. Although it succeeds maintaining control, as seen in Figure 5 left, the vehicle yaw rate starts to oscillate with an amplitude of 0.2deg/s at around t = 2s. The oscillation in the lateral acceleration has an amplitude of 0.06g, which might cause an unpleasant sensation to the driver.

Moving forward, the ramp steer maneuver serves to analyze the vehicle behavior in an almost steady state condition. The vehicle response can be understood with the plot of the steering angle vs. the lateral acceleration. The inclination of the curve is the understeer gradient K_u in deg/g. A higher inclination means a higher steering wheel input is necessary to achieve the same lateral acceleration. A lower inclination means the car is more responsive to steering input. The tests were performed at 60 km/h with a 6 deg/s steer increase, and 90 km/h with a 3 deg/s input.

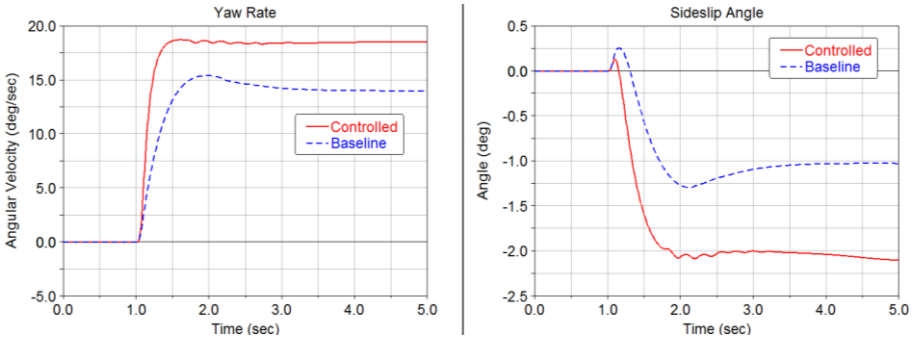

Fig. 5. Yaw Rate and Sideslip Angle in 90 km/h high lateral acceleration step steering

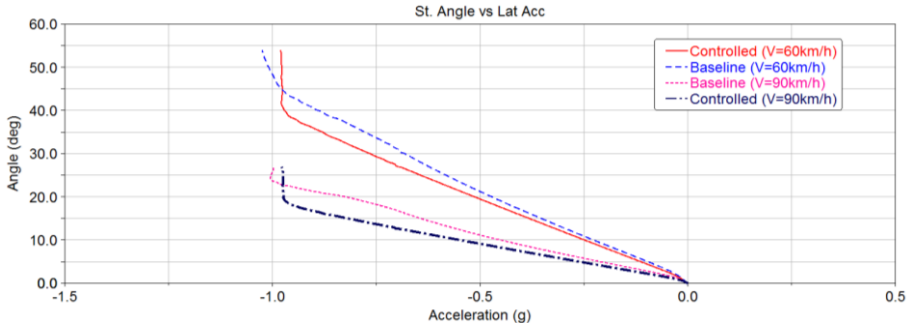

Fig. 6. Steering angle vs. Lateral acceleration in 60 km/h (bellow) and 90km/h (above) ramp steer

While both vehicles start with the same response, after lateral acceleration increases beyond a_y = 0.3g, the baseline vehicle starts having a more pronounced understeer behavior. After a_y = 0.5g the curve stops being linear and at 1g the car is at the grip limit. The controlled vehicle has a lower understeer gradient and a linear behavior up to the limit. This is especially good for the driver, which can correctly predict the car response and better control it. At almost a_y = 1g, the controller reference saturates, as explained in Equation 3. The reference yaw rate becomes constant and so the controller introduces terminal understeer. For the driver, this may be perceived strangely, as a turn of the steering wheel will not provide any lateral movement to the car (however, safer than rolling over).

A problem of this approach is the saturation employed in the controller depends on the tire-road friction coefficient μ. If on a higher grip surface, the controller will behave conservatively, limiting the car when it is still far away from its limits. If on a slippery surface, it may limit the car too late when the limit has already passed. To avoid such issues, an estimator for μ can be used.

The controller performance was also assessed in the double lane change maneuver with the goal of evaluating the handling of the vehicle. The maneuver was done at 75km/h and the throttle was applied throughout the simulation as to maintain the same initial speed. Because this is a closed loop simulation, in which the vehicle should follow a given trajectory, the steering control was done with the Adams Car Driving Machine. The Driving Machine uses one of four available modes to control the steering wheel: rotation or torque on the steering wheel, force or displacement in the steering rack. In the baseline vehicle, a torque control mode was used by the Driving Machine whereas in the controlled vehicle a rotation control mode was used.

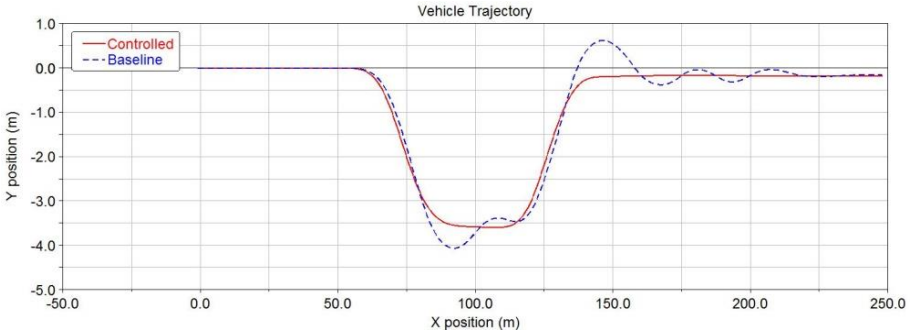

Fig. 7. Vehicle trajectory in double lane change at 75 km/h

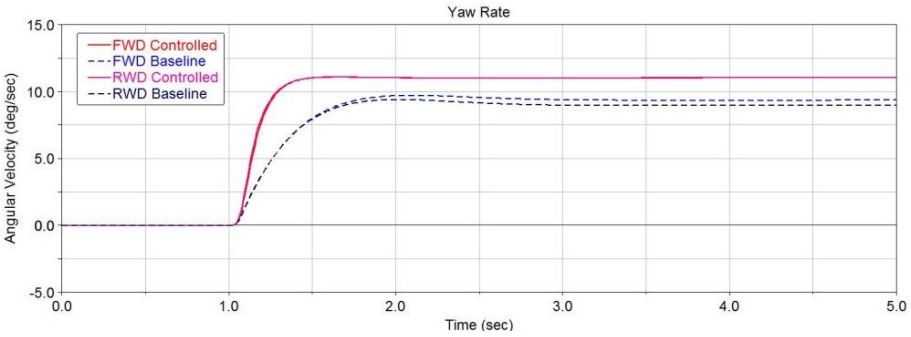

Fig. 8. Yaw rate of FWD and RWD in 90 km/h step steering

The baseline vehicle is almost not able to perform the test. From the trajectory plot, it is clear there are high overshoots in both turns and the settling time is very high. On the other hand, the controlled vehicle is able to successfully complete the maneuver without any troubles and with a much faster settling time, indicating that the higher responsiveness and lower understeering showed by the step steering and ramp steering can effectively improve dynamic response in a more complex situation.

Simulations were also done to investigate the behavior of the vehicle and the controller in an FWD or RWD configuration.

To change the vehicle from AWD to FWD/RWD, the in-wheel motors in the particular axle were removed. This had some effects on the vehicle: mass redistribution between the front and rear axles; changing in the wheels inertia, and the controller action to act only on the driving axle. The step steer test was simulated at 90km/h with steering wheel angle inputs of 9deg.

It is possible to compare the responses in terms of yaw rate. Both baseline RWD and FWD respond similarly, achieving almost the same steady-state value (9deg/s) in a similar settling time (approximately 1s). At this condition, the traction forces on the tires are not yet big enough to impact the lateral force generation and thus, alter the vehicle behavior. The controller is able to successfully stabilize the vehicle, increasing agility (new response time of 0.5s) and increasing the steady-state value of the yaw rate to more than 11deg/s in a similar way to the AWD vehicle. This shows the control strategy is robust to the configuration changes.

4 Conclusions

The objective of this article was to model an electric vehicle with IWMs, propose a torque vectoring controller that takes advantage of the individually controlled motors and assess its performance in different maneuvers. The vehicle was modeled in the multi-body dynamics software *Adams Car* in a co-simulation environment with *MATLAB*. The model works in open and closed maneuvers with a specifically tuned PI controller. A yaw rate based approach was used with the goal to improve vehicle response (make it more linear and responsive) and stability (avoid rolling over and critical conditions, such as drifting or spinning out) in different operating conditions. The controller is able to successfully alter vehicle response and make it better for the driver. On quasi steady-state conditions, the controller extends the linear range of the vehicle and stabilizes it at the limit. On transient conditions, such as step steer or the double lane change, steering wheel effort is greatly reduced as are overshoots of yaw rate. Also, settling time is lower, which means vehicle responds quicker to the steering commands. As the controller takes into account only yaw rate, it is important to observe the impact it has on vehicle side slip angle β. In the tested scenarios, the controller did not increase β values to unacceptable levels, assuming it had a correct estimation of μ. In different configurations, such as FWD or RWD, the controller proved to remain successful. With the same gains for all configurations, it was possible to obtain a satisfactory performance and improvement of vehicle response and minimize the influence of the tractive force on the front/rear axle, which could induce under/oversteer.

Further work can be done to improve and expand what has already been done: performing physical validation of subsystems and full vehicle test, with and without HIL; simulating the interaction with Traction Control Systems, ABS and ESC; optimizing control gains and torque allocation aiming to improve dynamic performance and/or reduce energy utilization; and a integrating a μ estimator to create a more robust control system.

Acknowledgements for Joao Pedro Almeida Viana for the important help during the modelling phase and MSC Software Italy for providing the Adams Car software and MSC technical team, particularly Ing. Angelo Casolo, for the active support during all the activity.

References

1. Carello, M., Ferraris, A., Airale, A., Fuentes, F.: City Vehicle XAM 2.0: Design and Optimization of its Plug-In E-REV Powertrain. SAE International Congress, Detroit (Michigan) 8-10 April, pp. 11, (2014), doi 10.4271/2014-01-1822.
2. Brusaglino, G., Buja, G., Carello, M., Carlucci, A.P., Onder, C.H., Razzetti, M.: New technologies demonstrated at Formula Electric and Hybrid Italy 2008. 24th International Battery, Hybrid and Fuel Cell Electric Vehicle Symposium and Exhibition EVS24, Stavanger (Norway), 13-16 May (2009)
3. Cubito, C., Rolando, L., Ferraris, A., Carello, M., Millo, F.: Design of the control strategy for a range extended hybrid vehicle by means of dynamic programming optimization. IEEE Intelligent Vehicles Symposium (IV), Los Angeles, CA, USA 11-14 June, pp. 1234–1241 (2017), ISBN: 978-1-5090-4804-5, doi: 10.1109/IVS.2017.7995881

4. Cittanti, D., Ferraris, A., Airale, A., Fiorot, S., Scavuzzo, S., Carello, M.: Modeling Li-ion batteries for automotive application: A trade-off between accuracy and complexity. International Conference of Electrical and Electronic Technologies for Automotive Torino. 15-16 June, pp. 8, (2017). ISBN: 978-88-87237-26-9, doi: 10.23919/EETA.2017.7993213
5. Scavuzzo, S., Guerrieri, R., Ferraris, A., Airale, A.G., Carello, M.: Alternative Efficiency Test Protocol for Lithium-ion Battery. International Conference on Environment and Electrical Engineering and 2018 IEEE Industrial and Commercial Power Systems Europe, EEEIC/I. Palermo, 12-15 June (2018).
6. Novellis, L.D., Sorniotti, A., Gruber, P., Pennycott, A.: Comparison of Feedback Control Techniques for Torque-Vectoring Control of Fully Electric Vehicles. IEEE Trans. Veh. Technol. 63, 3612–3623 (2014). doi:10.1109/TVT.2014.2305475
7. Carello, M., Airale, A., Ferraris, A., Messana, A.: XAM 2.0: from Student Competition to Professional Challenge. Comput.-Aided Des. Appl. 11, S61–S67 (2014). doi:10.1080/16864360.2014.914412
8. Gillespie, T.D.: Fundamentals of Vehicle Dynamics. Society of Automotive Engineers (1992)
9. Stoop, A.W.: Design and Implementation of Torque Vectoring for the Forze Racing Car. (2014)
10. Tahami, F., Kazemi, R., Farhanghi, S., Samadi, B.: Fuzzy Based Stability Enhancement System for a Four-Motor-Wheel Electric Vehicle. Presented at the SAE 2002 Automotive Dynamics & Stability Conference and Exhibition (2002)
11. Ghosh, J., Tonoli, A., Amati, N.: A Torque Vectoring Strategy for Improving the Performance of a Rear Wheel Drive Electric Vehicle. In: 2015 IEEE Vehicle Power and Propulsion Conference (VPPC). pp. 1–6. IEEE, Montreal, QC, Canada (2015)